Quasicritical heat capacity at a smectic-*A*–hexatic-*B* phase transition

H. Haga,[1] Z. Kutnjak,[2] G. S. Iannacchione,[1] S. Qian,[3] D. Finotello,[3] and C. W. Garland[1]
[1]*School of Science and Center for Material Science and Engineering, Massachusetts Institute of Technology, Cambridge, Massachusetts 02139*
[2]*Jozef Stefan Institute, 1001 Ljubljana, Slovenia*
[3]*Department of Physics, Kent State University, Kent, Ohio 44242*
(Received 5 March 1997)

High-resolution ac calorimetry has been used to characterize the excess heat capacity $\Delta C_p(T)$ associated with the smectic-*A* (Sm*A*) –hexatic-*B* (Hex*B*) transition in *n*-hexyl-4′-*n*-pentyloxybiphenyl-4-carboxylate (65OBC). For temperature oscillations in the investigated frequency range 1.42–400 mHz, the ΔC_p data reveal no frequency dependence and correspond to static thermodynamic values. The present data resolve several discrepancies in previously reported C_p values. This transition is *very* weakly first order, but power-law fits could be made to ΔC_p. Such fits yield an effective critical exponent $\alpha_{\rm eff}=0.65\pm0.05$, which agrees quite well with values of ~ 0.6 reported by Huang and co-workers [Phys. Rev. Lett. **46**, 1289 (1981); Phys. Rev. A **28**, 2433 (1983); Phys. Rev. Lett. **56**, 1712 (1986)]. Such an exponent value disagrees strongly with the theoretically predicted three-dimensional *XY* value $\alpha_{XY}=-0.007$. It is proposed that this C_p behavior and also the reported order parameter variation, which yields an effective critical exponent $\beta_{\rm eff}$ of ~ 0.2, are consistent with *quasitricritical* or *quasitetracritical* (strain-smeared, very weak first-order) behavior arising from a coupling between the amplitude of the bond-orientational order and the in-plane positional strain.
[S1063-651X(97)05908-4]

PACS number(s): 64.70.Md, 64.60.Fr, 65.20.+w

I. INTRODUCTION

The critical behavior of bulk liquid crystals at smectic-*A* (Sm*A*) –hexatic-*B* (Hex*B*) phase transitions is a challenging problem that is still not well understood. The conventional model of a bulk hexatic proposed in 1978 is a three-dimensional (3D) stack of weakly coupled 2D hexatic layers [1]. Such hexatic liquid crystals exhibit long-range bond-orientational (BO) order, but only short-range in-plane positional order, and the BO order parameter $\Psi=|\Psi|\exp(i6\psi)$ has *XY* symmetry, although it differs from the *XY* order parameter for helium superfluid or smectic-*C* liquid crystals since the azimuthal phase is not infinitely degenerate. Structural information on the Hex*B* phase, which was first obtained by a high-resolution x-ray-diffraction study of *n*-hexyl-4′-*n*-pentyloxybiphenyl-4-carboxylate (65OBC) [2], is consistent with this description and leads one to expect 3D *XY* universality for the critical fluctuation behavior at the Sm*A*-Hex*B* transition.

In contrast to the expectation of 3D *XY* critical behavior, almost all properties investigated near T_c deviate markedly from this prediction. For example, birefringence data on 65OBC yield an effective order parameter critical exponent $\beta_{\rm eff}=0.19\pm0.03$ [3] and heat capacity data on 65OBC yield the effective exponent $\alpha_{\rm eff}=0.60\pm0.03$ [4]. These values differ greatly from the 3D *XY* critical exponents $\alpha_{XY}=-0.007$ and $\beta_{XY}=0.345$ [5]. Indeed, Huang and Stoebe [6] have given an extensive review of the thermal properties of many stacked hexatic phases and conclude that numerous Sm*A*-Hex*B* experiments fail to conform to 3D *XY* universality. In particular, $\alpha_{\rm eff}$ values in many hexatic materials lie in the range 0.48–0.65.

The present work involves a high-resolution ac calorimetric reinvestigation of the Sm*A*-Hex*B* transition in 65OBC. There are two motivations for this study. Specific-heat values of 65OBC reported by Viner *et al.* [4(b)] at 1.74 Hz and those reported by Mahmood *et al.* [7] at 17 mHz differ significantly: the reported low-frequency excess heat capacity ΔC_p associated with the Sm*A*-Hex*B* transition has an appreciably larger amplitude than that reported at higher frequency and the effective critical exponent reported in Ref. [7] is larger than the value $\alpha=0.60$ given in Ref. [4(b)]. This apparent frequency dispersion in C_p indicates the possibility of dynamics at the Sm*A*-Hex*B* transition. Indeed, a complex frequency-dependent heat capacity $C_p^*(\omega,T)$ has been reported at a smectic-*C* (Sm*C*) –smectic-*I* (Sm*I*) critical point [8], which is the tilted analog of a Sm*A*–Hex*B* second-order transition.

The experimental results in Sec. II describe the behavior of C_p as a function of temperature and frequency (over the frequency window 1.42–400 mHz) near the Sm*A*-Hex*B* transition. An analysis of the data shows that the excess specific heat ΔC_p is a frequency-independent real quantity that corresponds to the static thermodynamic value. Indeed, there is no intrinsic frequency dependence of ΔC_p from 1.42 mHz to 1.74 Hz. This Sm*A*-Hex*B* transition is, however, *very weakly* first order. Section III shows that a power-law analysis can still be made and the effective ΔC_p critical exponent is $\alpha_{\rm eff}=0.65\pm0.05$. The discussion in Sec. IV comments on this $\alpha_{\rm eff}$ value and on a small secondary C_p feature that appears just below T_c. It is proposed that the critical behavior of C_p is consistent with quasicriticality arising from a coupling of Ψ with in-plane positional strains.

II. EXPERIMENTAL METHOD AND RESULTS

The structural formula and phase transition sequence on cooling for 65OBC ($M=368.5$ g mol^{-1}) are [2,4]

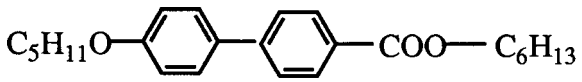

CrK — CrE — HexB — SmA — I
~329 K 334 K 340.5 K 358 K

where Cr*E* represents the plastic crystal-*E* phase with herringbone order and Cr*K* is a rigid crystalline phase that is presumably the stable phase at room temperature. It should be noted that the Cr*E*-Hex*B* and Cr*K*-Cr*E* transitions are monotropic since Cr*K* melts into the Hex*B* phase at 338 K.

Many measurements were made on samples from the same synthetic batch. For measurements made at MIT, a small mass of 65OBC (from 4.2 to 34 mg) was cold-weld sealed into a silver cell. The high-resolution ac calorimeters, which operate with an oscillating heat input $P_{\rm ac}\exp(i\omega t)$, have been described elsewhere [9,10]. One of the calorimeters was modified so that multiple $C_p(\omega)$ measurements could be made at a series of ω values at a constant (± 0.1 mK) temperature. The temperature was then changed by a small increment (~ 3.5 mK near T_c) and the $C_p(\omega)$ measurements repeated. Another calorimeter was used to measure $C_p(\omega)$ at fixed frequencies as a function of temperature, using a slow scan rate of ± 50 mK/h far from T_c and -10 mK/h near T_c for cooling run 10c. A variety of cell geometries were used. All cells were silver with a diameter of 1 cm; one cell was 1 mm thick with a helical coil of gold wire inserted to enhance the internal thermal conductivity and help to reduce or eliminate temperature gradients within the liquid crystal, one was 0.5 mm thick and filled with 65OBC without gold wire, and one was 0.5 mm thick but contained only an ~ 0.1-mm-thick layer of 65OBC and an ~ 0.4-mm air gap. The data that are most extensively analyzed were obtained with this last cell on cooling run 10c. For measurements made at Kent State, the cell and sample configuration was markedly different. The cell consisted of a thin sapphire disk, 1 cm in diameter and 0.1 mm thick, with a 50-Ω evanohm heater and 10-kΩ carbon flake thermistor securely attached to its underside with GE varnish. A 6.1-mg 65OBC sample was melted and spread over the top side of the sapphire disk. The sample's thickness was estimated to be ~ 0.1 mm over much of the disk. This allowed operation free from high-frequency rolloff up to ~ 100 mHz. The applied sinusoidal power was minimized to maintain $T_{\rm ac} \approx 3$ mK (zero-to-peak value) and temperature was scanned in a stepwise fashion with steps ranging from 50 mK away from the transition to $\lesssim 5$ mK near the transition. Further details are given in Ref. [11].

The standard frequency $\omega_0 = 0.196\ {\rm s}^{-1}$ used in most previous work at MIT corresponds to an ac temperature oscillation period of 32 s or a frequency $\omega_0/2\pi$ of 31.25 mHz. Data were obtained on 65OBC at MIT over the frequency range $\omega_0/22 - 2\omega_0$ ($f = 1.42 - 62.5$ mHz) and at Kent State over the range $f = 40 - 400$ mHz. MIT cooling runs were carried out starting at ~ 347 K in the Sm*A* phase; Kent State cooling runs started at ~ 360 K in the isotropic phase. Numerous heating runs were also made.

The thermal analysis equations that apply to the ac calorimetric data are [8,12]

$$|T_{\rm ac}| = \frac{|P_{\rm ac}|}{\omega C_t}\left[1 + \frac{1}{(\omega\tau_{\rm ext})^2} + \frac{(\omega\tau_{\rm int})^2}{90} + F\right]^{-1/2}, \quad (1)$$

$$\phi \equiv \Phi + \frac{\pi}{2} = \arctan\left[\frac{1}{\omega\tau_{\rm ext}} - \frac{\omega(\tau_s + \tau_c)}{\sqrt{90}}\right], \quad (2)$$

where Φ is the phase shift of $T_{\rm ac}$ with respect to $P_{\rm ac}$ and $C_t = C_s + C_c$, where C_s is the sample heat capacity and C_c is the empty cell heat capacity. The external relaxation time $\tau_{\rm ext} = RC_t$ characterizes heat flow from the sample to the surrounding thermal bath and the thermal resistance R is the reciprocal of the thermal conductance K_b to the bath. The internal relaxation time $\tau_{\rm int} = L^2/\sqrt{90}D_T$, where L is the sample thickness and D_T is its thermal diffusivity, characterizes the rate of heat flow through the sample and has a value for MIT cells from 0.015 to 0.35 s depending on the cell design. In the simplest one-lump model [12], $F = 2K_b/3K_s$, where K_s is the thermal conductance of the liquid crystal sample, and the quantities τ_s and τ_c are relaxation times C_s/K_s and C_c/K_c for the sample and the cell ($\tau_{\rm int}^2 = \tau_s^2 + \tau_c^2$). Unfortunately, high-frequency rolloff effects for the MIT cells are difficult to model over a large ω range, but Eqs. (1) and (2) will suffice up to $2\omega_0$ (62.5 mHz) if F is taken to be a *negative* ω-dependent but T-independent quantity [12]. These equations can be extended to cover the case where the heat capacity is a complex quantity $C_i = C_{\rm filled} = C'(\omega) - iC''(\omega)$, in which case [8]

$$C'(\omega) = \frac{|P_{\rm ac}|}{\omega|T_{\rm ac}|}\cos\phi, \quad (3)$$

$$C''(\omega) = \frac{|P_{\rm ac}|}{\omega|T_{\rm ac}|}\sin\phi - \frac{1}{\omega R}, \quad (4)$$

when $\omega\tau_{\rm int} \ll 1$ and $|F| \ll 1$ so that no corrections for internal gradients is required. For a pure real heat capacity,

$$C_p = [C'_{\rm filled}(\omega, T) - C_{\rm empty}]/m, \quad (5)$$

$$C''_{\rm filled} = 0, \quad (6)$$

where $C_{\rm empty}$ is the heat capacity of the empty cell (determined at ω_0) and m is the mass of 65OBC in grams. For most of the data obtained, $\omega\tau_{\rm int} \ll 1$ and $|F| \ll 1$ are excellent approximations and Eqs. (3)–(6) were used to reduce the $|T_{\rm ac}|$ and ϕ observables to C_p values. For MIT data obtained at $f \geqslant 25$ mHz, it was necessary to use Eqs. (1) and (2) to make small corrections (less than 1.6% for ω_0 and 4% for $2\omega_0$) for high-frequency rolloff effects (i.e., $\omega^2\tau_{\rm int}^2$ and F were not negligibly small, but luckily these terms were slowly varying with temperature). For Kent State data obtained at 150–400 mHz, Eqs. (1) and (2) were used with $F = 2K_b/3K_s$ to correct for small (less than 4%) high-frequency rolloff effects.

Overviews of the temperature dependences of C_p and ϕ at 10.4 mHz ($\omega_0/3$) are given in Fig. 1 for the range 332–347 K [13]. The first-order Hex*B*-Cr*E* freezing transition was seen at 334.62 K, as expected from Ref. [4(b)] where hysteresis was reported, and no further analysis or discussion of this transition will be given. The data shown in Fig. 1 were

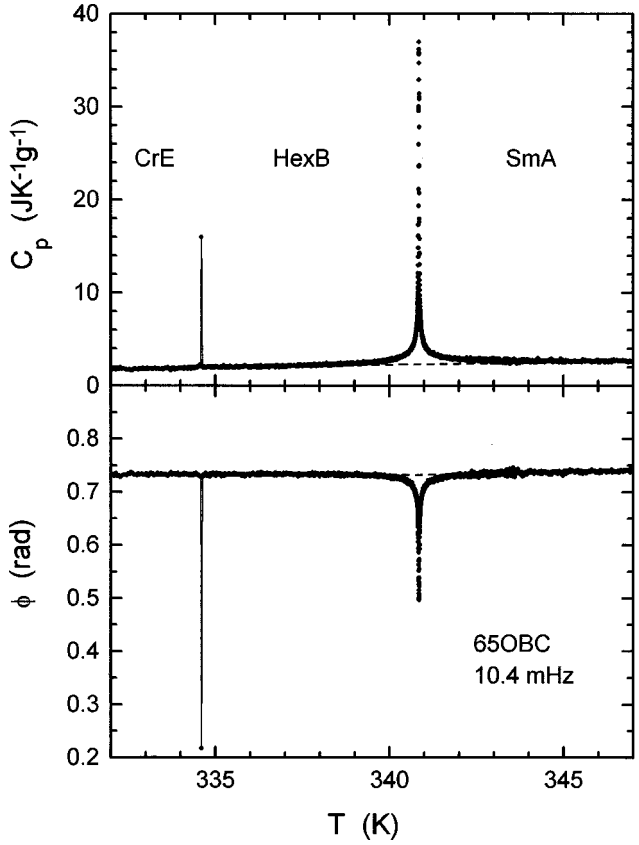

FIG. 1. Heat capacity C_p and phase shift ϕ observed for 65OBC with an ac calorimeter operated at $\omega=\omega_0/3$ (frequency $f=10.4$ mHz). $\phi\equiv\Phi+\pi/2$, where Φ is the phase shift of $T_{\rm ac}$ with respect to $P_{\rm ac}$. The dashed lines represent the noncritical background heat capacity and the base line for the phase shift ϕ. See Ref. [13] for information about the CrE-CrK transition.

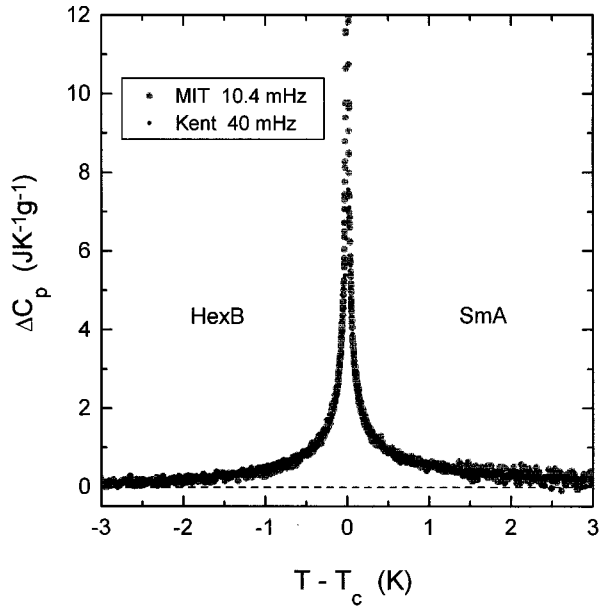

FIG. 2. Excess heat capacity ΔC_p associated with the SmA-Hex$B$ transition. Data sets obtained at MIT and Kent State are superimposed. Note that the MIT data are truncated and ΔC_p values from 12 to $\sim$35 J K^{-1} g^{-1} are not shown. A very small ''shoulder'' feature in the MIT data is not visible on this scale; see Fig. 7.

obtained on cooling run 10c, but excellent agreement was observed in the range T_c(SmA-Hex$B$)$\pm$5 K on a subsequent heating run at a scan rate of $+50$ mK/h. No frequency dependence was observed at any temperature for the MIT C_p data over the range $f=1.42-62.5$ mHz, although there is a narrow temperature range from $T_c-0.0095$ K to $T_c-0.037$ K, where a small history-dependent shoulder complicates the situation. No frequency dependence was observed in the Kent State C_p data over the range $f=40-400$ mHz. For the latter data, the resolution very close to T_c was not good enough to distinguish the presence or absence of the small shoulder feature.

There is calorimetric evidence that the 65OBC transition is *very weakly* first order: a hysteresis of $\sim$1 mK was observed and the $C_p(T)$ data within $\pm$10 mK of T_c differed in a small but systematic way on heating and cooling. Furthermore, phase shift data to be described below suggest a two-phase coexistence region from $T_c-0.2$ to $T_c+0.01$ K. The fact that any latent heat must be extremely small was confirmed by a nonadiabatic scanning run (linear-ramp relaxation method [8,14]), which measures total enthalpy changes (integrated C_p wings plus latent heat) and agreed well with the ac C_p data. The integrated excess enthalpy associated with the SmA-Hex$B$ transition is 4.95 ± 0.03 J g^{-1}, as determined by ac calorimetry. The total enthalpy from nonadiabatic scanning is the same within ±0.05 J g^{-1}. Thus the latent heat ΔH must be less than 0.05 J g^{-1}.

The excess heat capacity ΔC_p associated with the SmA-Hex$B$ transition was obtained from

$$\Delta C_p = C_p - C_p(\text{background}), \tag{7}$$

where C_p(background)$=B_r+E(T-T_c)$ represents the noncritical heat capacity that would be observed in the absence of the transition. This background term is given by the dashed line in Fig. 1 and a comparable line for the Kent State C_p data. For the MIT data, C_p(background)$=2.320+0.0554(T-T_c)$ in J K^{-1} g^{-1} units; C_p(background)$=2.134+0.0257(T-T_c)$ J K^{-1} g^{-1} for the Kent State data. Typical ΔC_p data sets from MIT and Kent State are shown in Fig. 2 over the range $|T-T_c|\leq3$ K. With *no adjustments* in the magnitude of these ΔC_p values, the overlay of the two data sets is essentially perfect. The only differences occur when T is very close to T_c($T_c-0.1$ to $T_c+0.02$ K), which is obvious from the fact that the maximum value of ΔC_p is 7.5–12 J K^{-1} g^{-1} in the Kent State data and $\sim$35 J K^{-1} g^{-1} in the MIT data. This difference, due largely to the lower density of Kent State points near T_c, is of no consequence for our data analysis.

Figure 3 compares the present ΔC_p data with values obtained from the ac calorimetric C_p data of Viner *et al.* [4(b)], which were obtained on a very thin cell (20 μm of liquid crystal) at 1.74 Hz and exhibited no frequency dependence over the range 0.65–1.74 Hz. We used a C_p(background) line taken from the data given in Ref. [4(b)], and this was determined to be $6.38+0.0320(T-T_c)$ J K^{-1} g^{-1} on the assumption that the liquid-crystal density is 1.0 g cm^{-3}. Clearly, the large B_r value of 6.38 is physically unreasonable, but that has no effect on the shape of the $\Delta C_p(T)$ curve. As shown in Fig. 3, a scaled version of ΔC_p(Viner)

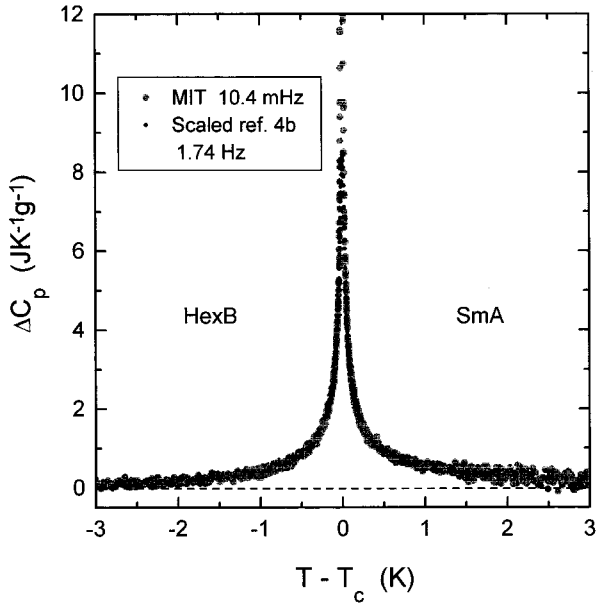

FIG. 3. Comparison of ΔC_p(SmA-Hex$B$) data for 65OBC obtained at $f=10.4$ mHz with *scaled* ΔC_p values at $f=1.74$ Hz from Ref. [4(b)]. In the latter case, the quantity shown is $1.35\Delta C_p$ [4(b)]; see the text.

matches our ΔC_p data extremely well. The ΔC_p(Viner) data were systematically smaller than the present ΔC_p values by a factor of $1/1.35=0.74$. Even with this scaling up of ΔC_p(Viner) values, the scaled maximum value of $\sim 8.5\ \mathrm{J\,K^{-1}\,g^{-1}}$ is far smaller than the MIT maximum of $\sim 35\ \mathrm{J\,K^{-1}\,g^{-1}}$.

The 65OBC heat capacity data at 17 mHz reported by Mahmood *et al.* [7] only cover the range $T_c-1.6$ to T_c+1 K. This is too narrow a temperature range to allow an unambiguous choice of a C_p(background) line from the Ref. [7] data. We have *arbitrarily* chosen the line $C_p(\mathrm{background})=2.50-0.0347(T-T_c)\ \mathrm{J\,K^{-1}\,g^{-1}}$ in order to achieve the best match between our ΔC_p data and scaled ΔC_p(Mahmood) values. Although this B_r value of 2.50 is quite reasonable physically and agrees well with the MIT and Kent State values, a negative value for the slope E is unexpected and suspect unless it arises from some instrumental effect such as a slightly incorrect calibration of the thermometer (thermocouple). With this choice of C_p(background), a scaled version of ΔC_p(Mahmood) matches our ΔC_p data as well as the $1.35\Delta C_p$(Viner) data shown in Fig. 3. In the case of Ref. [7], the ΔC_p(Mahmood) data were systematically larger than the present ΔC_p values by a factor of 1.61, i.e., $0.62\Delta C_p$(Mahmood) overlays our data extremely well. Note that the unscaled maximum value of ΔC_p(Mahmood) is $16.9\ \mathrm{J\,K^{-1}\,g^{-1}}$ and the scaled maximum is $10.5\ \mathrm{J\,K^{-1}\,g^{-1}}$.

The conclusions to be drawn from Figs. 2 and 3 plus the discussion above of ΔC_p (Mahmood) is that four completely independent ac calorimetric studies on three different good-quality 65OBC samples all yield the *same shape* for $\Delta C_p(T)$. The major difference between previously published C_p data on 65OBC [4,7] appears to lie in systematic multiplicative errors in the absolute magnitude of the peak. One comparison relevant to sample quality is the *absolute* values

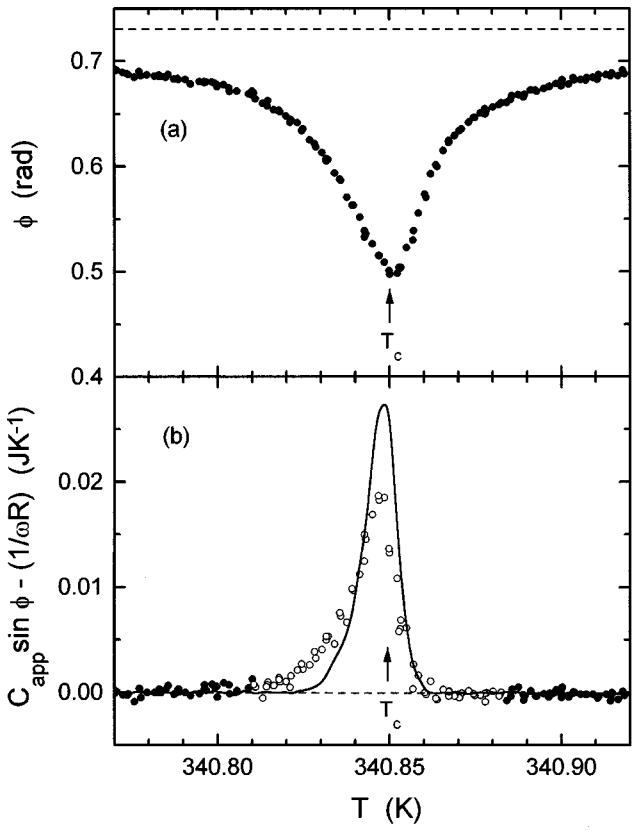

FIG. 4. (a) Phase shift ϕ observed for 65OBC in run 10c near T_c at $f=10.4$ mHz. The dashed line is the same as that shown in Fig. 1. (b) The quantity $C_{\mathrm{app}}\sin\phi-1/\omega R$ should be zero if the heat capacity of cell plus sample is a pure real quantity, there is no two-phase coexistence, and there are no high-frequency effects associated with internal temperature gradients. C_{app} is defined as $|P_{\mathrm{ac}}|/\omega|T_{\mathrm{ac}}|$ and R is the thermal resistance (inverse conductance) of the link between the sample cell and the thermal bath. The open circles correspond to C_p run 10c data points that were not used in the fitting procedure. The smooth curve represents the behavior observed in a later run 11c.

for T_c in the four experimental studies. Viner *et al.* [4(b)] report $T_c=340.44$ K [values of 340.73 and 341.08 K have also been reported for other C_p studies by Huang's group [4(a),4(c)]] and the uncertainty in the absolute accuracy appears to be ± 0.2 K [4(a)]; data from Mahmood *et al.* [7] yield 340.935 K (no absolute accuracy cited); the MIT value is $T_c=340.85\pm 0.2$ K; and the Kent State value is $T_c=341.02\pm 0.3$ K. Note also that the MIT sample was very stable: a very small T_c drift of -0.125 mK/d was observed over the first 8 d, but three runs over the subsequent 7 d showed no T_c drift within our resolution of better than ± 1 mK.

Before undertaking an analysis of the ΔC_p data, we wish to present detailed phase shift data for MIT run 10c, which is the cooling run at 10.4 mHz shown in Figs. 1–3. Figure 4(a) shows the temperature dependence of ϕ near T_c. This is a detailed view of the data in Fig. 1, and the dashed line in Fig. 4(a) is the same as that in Fig. 1. Although it is known that a dip in ϕ is a characteristic of second-order transitions, the significant fact here is that the ϕ dip very close to T_c is not large enough to be consistent with second order. As a quan-

TABLE I. Least-squares values of the adjustable parameters for fitting ΔC_p data of run 10c with Eq. (8). The ΔC_p data were obtained from C_p values measured at 10.4 mHz and $C_p(\text{background}) = 2.320 + 0.0554(T - T_c)$ J K^{-1} g^{-1}. Quantities held fixed during a fit are enclosed in square brackets. Range *A* (410 points) has $|t|_{\max} = 10^{-3}$, range *B* (688 points) has $|t|_{\max} = 3\times10^{-3}$, range *C* (942 points) has $|t|_{\max} = 6\times10^{-3}$, range *D* (1161 points) has $|t|_{\max} = 10^{-2}$, and range *E* (1322 points) has $|t|_{\max} = 1.5\times10^{-2}$. In all fits, $|t|_{\min} \simeq 1.1\times10^{-4}$. The units of $A^{\pm}$ and $B_c^{\pm}$ are J K^{-1} g^{-1}. The estimated standard deviations σ for ΔC_p points are shown in Fig. 5.

Fit	Range	T_c (K)	α_{eff}	Δ	$100A^+$	A^-/A^+	D_1^+	D_1^-/D_1^+	B_c^+	B_c^-	χ_ν^2
1	*A*	340.848	0.645		1.653	1.014	[0]	[1]	−0.232	$[B_c^+]$	1.11
2	*B*	340.847	0.645		1.671	0.990	[0]	[1]	−0.229	$[B_c^+]$	1.22
3	*C*	340.848	0.656		1.495	1.001	[0]	[1]	−0.183	$[B_c^+]$	1.35
4	*D*	340.848	0.652		1.561	0.999	[0]	[1]	−0.198	$[B_c^+]$	1.54
5	*E*	340.848	0.651		1.569	0.997	[0]	[1]	−0.200	$[B_c^+]$	1.53
6	*A*	340.851	0.645		1.572	1.128	[0]	[1]	−0.130	−0.334	1.03
7	*B*	340.852	0.640		1.618	1.171	[0]	[1]	−0.121	−0.372	0.97
8	*C*	340.851	0.649		1.502	1.140	[0]	[1]	−0.104	−0.322	0.91
9	*D*	340.850	0.651		1.493	1.114	[0]	[1]	−0.114	−0.299	1.09
10	*E*	340.849	0.653		1.485	1.086	[0]	[1]	−0.122	−0.279	1.10
11	*C*	340.850	0.641	[0.75]	1.666	1.099	26.9	0.169	−0.381	$[B_c^+]$	0.92
12	*D*	340.850	0.657	[0.75]	1.416	1.097	−0.918	22.059	−0.095	$[B_c^+]$	1.10
13	*E*	340.849	0.655	[0.75]	1.469	1.068	5.51	−1.899	−0.171	$[B_c^+]$	1.11

titative indication of this, Fig. 4(b) shows the variation of $[C_{\text{app}}\sin\phi - (1/\omega R)]$, where the apparent filled cell heat capacity C_{app} is defined as $|P_{\text{ac}}|/\omega|T_{\text{ac}}|$. If internal gradient effects were negligible at all T for $f = 10.4$ mHz, the transition was second order (no two-phase coexistence), and the heat capacity C_p was a pure real quantity ($C'' = 0$), then the quantity plotted in Fig. 4(b) should be zero everywhere. $[C_{\text{app}}\sin\phi - (1/\omega R)]$ is zero over $T_c \pm 5$ K, except for the range from $T_c - 0.04$ to $T_c + 0.01$ K. The subsequent run 11c has an even smaller anomaly below T_c and the low-temperature C_p shoulder discussed later (see Fig. 7) has also decreased. We believe that the narrow region of anomalous phase behavior observed in run 11c indicates first-order two-phase coexistence, but the extra anomaly for run 10c is related to the low-temperature C_p shoulder.

III. DATA ANALYSIS

In order to avoid any misleading subtle anomalies in C_p near T_c associated with the anomalous ϕ behavior in Fig. 4(b) and also to avoid systematic perturbations in C_p values related to a finite amplitude for $|T_{\text{ac}}|$, data in the range 340.810–340.885 K were excluded from the fits to be presented below. Although the Kent State data agree very well with the MIT data (see Fig. 2), the data points are sparse very close to T_c and the Kent State data have not been analyzed.

Fits to ΔC_p data at 10.4 mHz were based on the empirical power-law form

$$\Delta C_p^{\pm} = A^{\pm}|t|^{-\alpha_{\text{eff}}}(1 + D_1^{\pm}|t|^{\Delta}) + B_c^{\pm}, \tag{8}$$

where $t = (T - T_c)/T_c$ is the reduced temperature and $B_c^{\pm}$ is a critical contribution to the regular (nonsingular) heat capacity behavior. A detailed discussion of the theoretical ΔC_p power-law expression expected and observed for 3D *XY* liquid-crystal systems is given in Ref. [15]. The critical C_p exponent is denoted as α_{eff} since the Sm*A*-Hex*B* data do not yield a value for α that corresponds to any presently known second-order universality class. Usually, the correction exponent Δ is the corrections-to-scaling exponent $\Delta_1 \simeq 0.5$. Note that if $\alpha_{\text{eff}} > 0.5$, the correction term $A^{\pm}D_1^{\pm}t^{\Delta_1 - \alpha_{\text{eff}}}$ will diverge at T_c rather than go to zero as it usually does. Thus we will explore also the purely empirical choice $\Delta = 0.75$ used in the analyses of Refs. [4] and [6]. The usual scaling constraint on B_c is $B_c^+ = B_c^-$.

Table I shows the fitting parameters obtained over five ranges of $|t|$ with three different fitting forms. Fits 1–5 are simple power-law fits with $B_c^+ \equiv B_c^-$ required. These fits yield $\alpha_{\text{eff}} = 0.65 \pm 0.05$, where the uncertainty represents 95% confidence limits obtained with the *F* test. The 95% limiting values of $F(\nu,\nu)$ are 1.22–1.11 for ranges *A*–*E*, respectively. These fits 1–5 are not too bad in quality, as indicated by the χ_ν^2 values, but there are small systematic trends to the residuals $\Delta C_p(\text{obs}) - \Delta C_p(\text{fit})$ as shown in Fig. 5(a). In order to improve the fits it is necessary to (a) allow $B_c^+ \neq B_c^-$ with $D_1^{\pm} = 0$, (b) allow $D_1^{\pm} \neq 0$ with $\Delta = \Delta_1 = 0.5$, or (c) allow $D_1^{\pm} \neq 0$ with $\Delta \equiv 0.75$. Fits 6–10 of type (a) are better fits than fits 1–5, as shown by the χ_ν^2 values and the residuals shown in Fig. 5(b), but α_{eff} still equals 0.65. Fits of type (b) are also better than fits 1–5 and comparable to fits 6–10 in quality. However, such fits are not listed in Table I since the D_1^-/D_1^+ ratios are *negative* for ranges *D* and *E*. This means that the correction term $A^{\pm}D_1^{\pm}|t|^{0.5-\alpha_{\text{eff}}}$ goes to $+\infty$ as $T \to T_c$ in the Sm*A* phase and goes to $-\infty$ as $T \to T_c$ in the Hex*B* phase, which does not seem physically plausible. Furthermore, both D_1^+ and the ratio D_1^-/D_1^+ are very unstable on range shrinking. In spite of these serious troubles, the average value of α_{eff} is 0.66 for such type (b) fits. Fits have even been carried out with $B_c^+ \equiv B_c^-$ and second correction terms $D_2^{\pm}|t|$ added to Eq. (8). Such fits were unphysical (although $D_1^-/D_1^+ \simeq 1$) since $A^{\pm}D_1^{\pm}|t|^{0.5-\alpha_{\text{eff}}}$ and B_c were large dominant contributions, but opposite in sign and roughly canceling each other.

Fits 11–13 are of type (c) above with $\Delta \equiv 0.75$ and $B_c^+ \equiv B_c^-$. Such fits were not made for ranges *A* and *B*, where $|t|_{\max} = 1\times10^{-3}$ and 3×10^{-3}, since the fitting procedure is

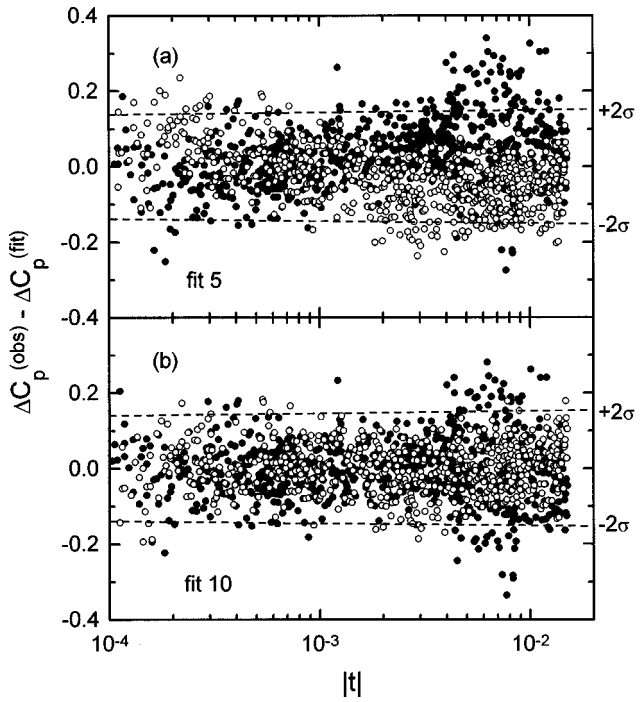

FIG. 5. (a) Plot of the residuals versus the reduced temperature t for fit 5, where σ is the estimated standard deviation. Note the systematic trends: the residuals for $T>T_c$ (●) change from slightly positive at $t=10^{-2}$ to slightly negative at $t=10^{-4}$ and the trends of the residuals for $T<T_c$ (○) are opposite to this. (b) Plot of the residuals versus t for fit 10.

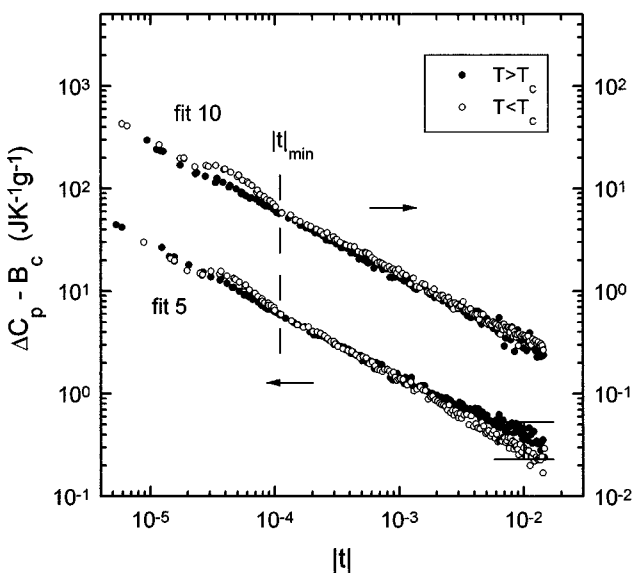

FIG. 6. Log-log plots of $\Delta C_p - B_c$ vs $|t|$ for 65OBC data at 10.4 mHz. The values of B_c are $B_c^+ = B_c^- = -0.200$ for fit 5 and $B_c^+ = -0.122$, $B_c^- = -0.279$ for fit 10. Both fits are based only on data where $|t| \geq 1.1\times10^{-4}$. Deconvolved points for $|t|<1.1\times10^{-4}$ are shown for completeness. A typical error bar for large $|t|$ is shown on the fit 5 plot; at $|t|\leq10^{-4}$ the error bars are smaller than the plotted points. See the text for further details.

very unstable when large correction terms are allowed for narrow $|t|$ ranges. The χ^2_ν values and residuals (not shown) for fits 11–13 are essentially the same as those for fits 8–10. This is not surprising since the principal role of the $A^{\pm}D_1^{\pm}|t|^{0.75-\alpha_{\rm eff}}$ terms is to act as a mimic function generating a rounded pseudostep. At $|t|_{\rm max}$, the average value of $A^+D_1^+|t|^{0.75-\alpha_{\rm eff}} - A^-D_1^-|t|^{0.75-\alpha_{\rm eff}}$ is 0.190 for ranges C–E (the ''step'' values range from 0.209 for C to 0.196 for D to 0.165 for E). The step $\Delta B_c = B_c^+ - B_c^-$ in fits 8–10 averages 0.187 (ranging from 0.218 for C to 0.185 for D to 0.157 for E). Furthermore, the value of the critical exponent ($\alpha_{\rm eff} \simeq 0.64$) for the fits 11–13 agrees well with the other fits. The greatest source of uneasiness about fits of type (c) is the very unstable behavior of D_1^+ and D_1^-/D_1^+ with range shrinking. In our view, such fits merely appear to avoid violations of scaling and are not theoretically more appealing than fits 6–10, where $\Delta B \neq 0$ violates scaling explicitly.

Log-log plots of $\Delta C_p - B_c$ versus $|t|$ are given for fits 5 and 10 in Fig. 6. Only points with $|t| \gtrsim 1.1\times10^{-4}$ were used in the fits, but points with $|t|<1.1\times10^{-4}$ have been added after a deconvolution correction was made as described below. Since very many points were available in the wings, the data shown in Fig. 6 have been merged for clarity and to reduce the random scatter. For $1.5\times10^{-3}<|t|<4\times10^{-3}$ nine adjacent points are merged and for $|t|>4\times10^{-3}$ eleven points were merged. For run 10c, the $|T_{\rm ac}|$ amplitude was 13.5 mK zero-to-peak far from T_c and $\sim$9 mK at $t=\pm2.5\times10^{-5}$ (or $T_c \pm 8.5$ mK), where $C_p \simeq 18$ J K^{-1} g^{-1}. This moderately large amplitude is desirable for improving the overall signal-to-noise ratio, but close to T_c it clearly causes the C_p values calculated with Eqs. (3) and (5) to be systematically too low. A deconvolution calculation was made using the least-squares fitting form and the measured $|T_{\rm ac}|$ values at every point close to T_c. The ac method yields an average C_p over a temperature window of width $2|T_{\rm ac}|$. Far from T_c, the C_p variation can be taken as linear over a narrow range and the $|T_{\rm ac}|$ amplitude has no effect on the value of C_p. However, if $\Delta T = T - T_c$ is small (possibly even smaller than $2|T_{\rm ac}|$) and C_p varies strongly with temperature, the method will yield a low value for C_p. By combining a trial fitting form, like $A|t|^{-\alpha}+B$, with the observed $|T_{\rm ac}|$ value at a point one can ''deconvolve'' the data and extract the underlying true C_p value that has been distorted by the finite $|T_{\rm ac}|$ used. The results of this deconvolution are shown in Figs. 6 and 7. The data points used for the fits of run 10c were outside the t range where the finite $|T_{\rm ac}|$ amplitude effect matters. In Fig. 7 such points are shown as filled circles, and open circles are the deconvolved points. Two features of run 10c are immediately obvious: (a) deconvolved points close to T_c fall on the fit curve very well for $T>T_c$ and (b) there is a small ''shoulder'' below T_c that lies between $t=-2.8\times10^{-5}$ ($\Delta T=-9.5$ mK) and $t=-1.1\times10^{-4}$ ($\Delta T=-37.5$ mK). This shoulder has an integrated area of $\sim$0.04 J g^{-1} for run 10c. Also shown in Fig. 7 are C_p data from an early run (run 4c, carried out at ω_0) and a later run (run 11c, carried out at $2\omega_0$). Both of these runs required small systematic corrections with Eqs. (1) and (2) for high-frequency rolloff due to finite $\omega\tau_{\rm int}$ and F effects. The run 4c and run 11c data points after high-frequency rolloff corrections and $|T_{\rm ac}|$ deconvolution are shown in Fig. 7 with the same fit-10 theory curve given for run 10c.

It should be stressed that the C_p shoulder is present in the raw data and is not an artifact related to the deconvolution procedure. Other runs in addition to those shown have dem-

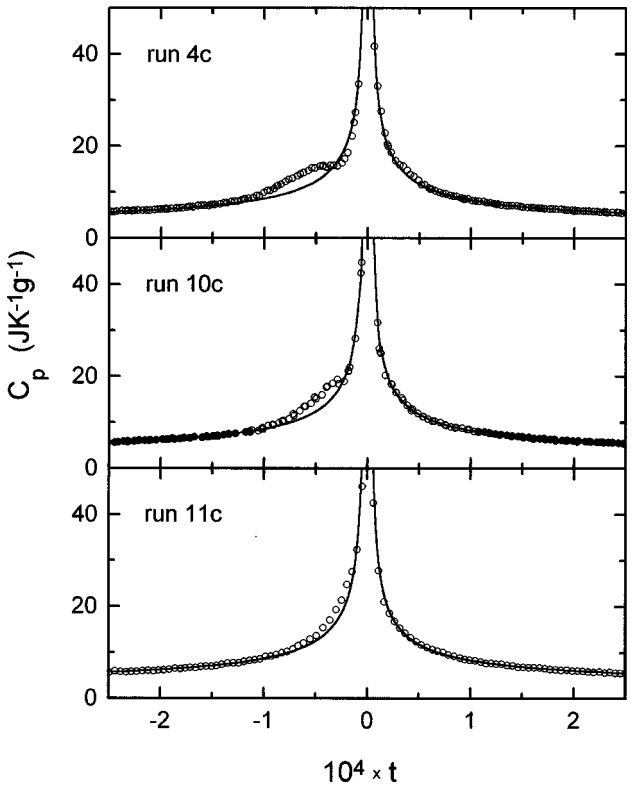

FIG. 7. C_p data for 65OBC obtained in three cooling runs at different times. The total time spent at high temperatures ($T > 335$ K) was 2 d for run 4c, 9 d for run 10c, and 13 d for run 11c. The run 10c data used for the fits in Table I are shown as filled circles; open-circle points in the gap $|t| < 1.1 \times 10^{-4}$ have been deconvolved to correct for any systematic effects of a finite $|T_{ac}|$ amplitude. Data for runs 4c and 11c have also been deconvolved where necessary (close to T_c). The smooth ''theory'' curves are the same in all three boxes and represent fit 10 given in Table I.

onstrated that the low-temperature shoulder feature is not sensitive to frequency but is time dependent. The size of this anomalous shoulder decreased monotonically with time at high temperatures (i.e., 337 K$\lesssim T \leqslant$347 K). In parallel with this decrease in the integrated area (enthalpy) of the shoulder, there was a slight but systematic increase in the maximum value of ΔC_p observed at T_c. Such changes were also mirrored in the behavior of the phase shift ϕ. As time spent at high temperatures increased, the anomalous $C_{app}\sin\phi - (1/\omega R)$ values below T_c decreased in size and in temperature range, while the peak values at T_c slightly increased; see Fig. 4. For runs 11c and a subsequent heating run 12h, the C_p shoulder is almost gone, as shown in Fig. 7, and the $C_{app}\sin\phi - (1/\omega R)$ anomaly narrowed to an almost symmetrical peak about 25–30 mK wide, as shown in Fig. 4. Note that essentially no changes occurred in the behavior of C_p or $C_{app}\sin\phi - (1/\omega R)$ for $T > T_c$. During the evolution of the C_p shoulder, its center position shifted very slightly from $T_c - 0.026$ K for early run 2c to $T_c - 0.018$ K for later runs 8c and 9h. The shoulder is too weak to allow an estimate of its position for runs 10c, 11c, and 12h. It should be noted that freezing of the Hex*B* phase into the Cr*K* phase at the end of run 10c did not cause the shoulder feature to increase in the subsequent runs 11c and 12h. We speculate that the shoulder, which was effectively annealed away by run 12h, would reappear if the sample were heated again into the isotropic phase, but that was not tried.

IV. DISCUSSION

The most important issue to discuss is the values of the critical exponents at the Sm*A*-Hex*B* transition in 65OBC. It has long been known [4,6,7] that the effective C_p exponent $\alpha_{eff} \simeq 0.60-0.64$ and the effective order parameter exponent is $\beta_{eff} \simeq 0.19$ [3]. These values are far from the 3D *XY* universal values and the possible influence of short-range herringbone orientational order [16] has been eliminated as a significant factor in *nm*OBC compounds [17]. The same effective BO order parameter exponents have also been observed in systems with the phase sequence Sm*A*-Hex*B*-Cr*B*, where there is no indication of even short-range herringbone order: $\beta_{eff} = 0.25$ and 0.20 in PIR5 and PIR7 (alkoxyphenylamino-methylpirydil-propenones) [18(a)] and $\beta_{eff} = 0.15 \pm 0.03$ for 1-4′-(fluorphenylamino)-3(4″-hexyloxyphenyl)-1-propene- 3-one (RFL6) [18(b)].

It is known from the multicritical scaling of C_{6n} order parameter harmonics [19,20] that the sixfold bond-orientation order parameter Ψ in the tilted Hex*I* phase of supercritical methylbutyl phenyl octyloxybiphenyl-carboxylate (8OSI) conforms to the 3D *XY* universality class and C_{6n} data for the Hex*B* phase of RFL6 seem to lie in a crossover region between mean field and 3D *XY* [18b]. However, it is also clear that the Sm*A*-Hex*B* enthalpy behavior is very closely linked to the in-plane positional behavior [18,21,22] rather than the phase behavior of Ψ. There is very little energy associated with fluctuations of BO order, but changes in the lateral nearest-neighbor distances will have a definite effect on the energy. In particular, temperature-dependent changes in the in-plane wave vector $q_0 = 2\pi/l$, where l is the lateral distance between molecules, and in the in-plane positional inverse correlation length κ are given by a theoretical model [21] as $\Delta q_0 \equiv q_0(T) - q_0(T_c) = |D|\langle|\Psi|^2\rangle \sim \mp A^{\pm}|t|^{1-\alpha}$, which is proportional to the negative of the excess critical enthalpy $H(T) - H(T_c)$ and $\Delta\kappa^2 = |B|\langle|\Psi|^2\rangle^{1/2} + C\langle|\Psi|^2\rangle$. Fits to positional powder x-ray data on 46OBC with this model are good and are reported [22] to yield $\alpha_{eff} = 0.49$ and a Δq_0 amplitude ratio consistent with the heat capacity amplitude ratio $A^-/A^+ = 1.3$, in agreement with results from Huang's group [23]. The theoretical coefficients B, C, and D arise from a Ψ density coupling term $F_{\Psi-\rho} = [B_q|\Psi|\cos 6(\theta - \psi) + C_q|\Psi|^2]|\rho_q|^2$ in the free energy with B_q taken as a constant $B < 0$ and C_q taken as $C + 2D(q - q_0)$ with $D < 0$ and C unspecified. Furthermore, $|\Psi|$ is replaced by $\langle|\Psi|^2\rangle^{1/2}$, so that amplitude fluctuation effects are not included. Near the transition, where $B_q^2\langle|\Psi|^2\rangle/[\kappa_0^2 + (q - q_0)^2 + C_q\langle|\Psi|^2\rangle] \ll 1$, the sixfold modulation would not appear as a significant feature in the structure factor S_q and the main effects of the coupling term are (a) a renormalization of T_c, (b) a ''magnetothermomechanics'' type effect from the $|\Psi|^2(q - q_0)$ strain coupling that links anomalous thermal contraction to the critical energy, analogous to that observed for order-disorder phenomena in NH_4Cl [24], and (c) an increase in the in-plane correlation length $\xi_{\|} = 1/\kappa$. The connection between enthalpy and in-plane positional behavior is supported by work on pentyl-pentanoyloxybiphenyl-carboxylate (54COOBC), which exhibits the sequence Sm*A*-Hex*B*-Cr*B*

and a weakly first-order bulk transition with SmA+Hex$B$ coexistence over ~ 90 mK [25(a)]. In two-layer films of 54COOBC the C_p peak is related to a dramatic increase in $\xi_\parallel$ without any sixfold modulation and no C_p peak occurs at the temperature (~ 3 K lower) where electron diffraction shows the onset of sixfold BO order modulation [25]. It should be noted that sharpening of the diffraction ring (indicating a substantial increase in $\xi_\parallel$) occurs at a temperature above that where sixfold modulation first appears in many materials that exhibit a Hex$B$ phase [25(c)]. Further evidence of the coupling of Ψ and positional variables is provided by the ultrasonic in-plane longitudinal sound velocity of 65OBC [26], which exhibits just the kind of dip at T_c that is seen in NH_4Cl, a prototypical compressible Ising system.

Our view is that one should focus on the in-plane positional aspects of the Ψ-ρ or Ψ-strain coupling and ignore for present purposes the behavior of the BO order phase ψ that gives rise to the sixfold fundamental modulation and its harmonics C_{6n}. It is physically reasonable that C_p depends more on the average lateral distance between molecules (van der Waals forces) than on the ''bond angles.'' This view is supported by suggestions made by Mahmood *et al.* [7]. Thus the problem becomes a compressible XY analog of the 3D compressible Ising problem that was solved by Bergman and Halperin [27]. For the compressible Ising lattice, fluctuations in strain driven by the fluctuations in the spin order parameter cause *quasitricritical* behavior (a very weak first-order instability but almost tricritical behavior) rather than the Ising behavior that would occur for a rigid lattice. This instability occurs for any compressible Ising lattice with a finite coupling coefficient (i.e., $dT_c/dp \neq 0$) since C_p for the bare Ising model goes to infinity at T_c ($\alpha > 0$), but a comparable instability should occur for an XY model with $\alpha_{\rm bare} < 0$ if the finite maximum in the bare C_p at T_c is large enough and the material is soft enough. The present work suggests that any underlying XY peak would be very large. Furthermore, it is known that dT_c/dp is large (~ 30 K/kbar) for the 65OBC SmA-Hex$B$ transition [28]. The only elastic difference between the Hex$B$ phase and a crystalline phase such as CrB is the absence of a static in-plane shear stiffness [29]. However, since the in-plane correlation length can be fairly large in a Hex$B$ phase there should be high-frequency phonon modes associated with the small ''crystallike'' rafts and thus local elastic shear stiffness.

In the case of a compressible strain-coupled model, one expects Gaussian behavior where the susceptibility exponent γ is 1, as seen in NH_4Cl [30]. The data in Ref. [3] indicate that $2\beta = 1 - \alpha$ for 65OBC within moderate error bounds of ± 0.05. If this result is valid, the scaling relation $\alpha + 2\beta + \gamma = 2$ yields $\gamma \simeq 1$, which would indicate a Gaussian SmA-Hex$B$ transition in 65OBC. Another general theoretical treatment of $|\Psi|^2$(strain) coupling between n-vector order parameters Ψ and elastic strain [31] includes an analysis of three-dimensional $n = 2$ (XY) systems and indeed the liquid-crystal SmA-SmC transition. In the latter case, the relevant coupling is between an XY order parameter and the *uniaxial strain normal* to the smectic layer and such coupling is predicted to have no effect on the constant pressure critical behavior at a SmA-SmC transition. For coupling of an XY order parameter to a 3D elastic continuum, the theory in Ref. [31] predicts that there are marginally relevant correction terms whose effect on the critical behavior is unknown but presumed to lead only to logarithmic corrections to scaling. However, a detailed treatment in the spirit of Bergman and Halperin has not been carried out for $|\Psi|^2$(strain) coupling where $|\Psi|$ is the XY order parameter amplitude and the strain is explicitly in-plane rather than isotropic. If SmA-Hex$B$ transitions have positional quasitricritical character, this would explain why a wide range of hexatic materials exhibit almost the same SmA-Hex$B$ heat capacity exponents since the key factor is the in-plane elastic stiffness not some field variable that tunes the free-energy coefficient of $|\Psi|^2$ to zero at a single point where the transition changes over from second order to first order in the usual way. Another comment about the role of elastic (or density) degrees of freedom in the SmA-Hex$B$ problem is to note that if the bare system were to be controlled by a new fixed point with $\alpha > 0$ (instead of the XY fixed point with $\alpha_{XY} = -0.007$), then $|\Psi|^2$ (strain) coupling should create instabilities and weak first-order behavior even more easily.

Let us now review the evidence that the SmA-Hex$B$ transition in 65OBC is very weakly first order. *First*, there is a tiny hysteresis of ~ 1 mK seen in both C_p and ϕ data on heating and cooling. *Second*, there is anomalous behavior in $C_{\rm app}\sin\phi - (1/\omega R)$ that is characteristic of two-phase coexistence over a (25–30)-mK-wide region about T_c. *Third*, the power-law fits are significantly improved if $B_c^+ > B_c^-$ is allowed as in our fits 6–10, which breaks scaling in a way compatible with a first-order transition. Note that fits of 65OBC data with $B_c^+ > B_c^-$ are also reported in Refs. [4(a), 4(b)] and [7]. *Fourth*, an apparently discontinuous jump in the in-plane correlation length $\xi_\parallel$ of ~ 11 Å was observed in Ref. [2]. The statement that the first-order character must be very weak is supported by the lack of a latent heat large enough to be detected within our resolution (see Sec. II) and the fact that quite good power-law fits can be achieved if $B_c^+ \neq B_c^-$ is allowed. Furthermore, a weak first-order character at SmA-Hex$B$ transitions in nmOBC homologs is supported by recent calorimetric work showing that 3(10)OBC definitely has a two-phase coexistence region, but the pretransitional C_p wings can be fit with a critical exponent $\alpha_{\rm eff} = 0.68 \pm 0.10$ [32].

The important question is why the observed $\alpha_{\rm eff}$ and $\beta_{\rm eff}$ values differ from the tricritical values of 0.5 and 0.25, respectively. One possibility for weakly first-order transitions in which the material contracts on ordering (smaller lateral nearest-neighbor distances in hexatic 65OBC) is strain smearing of the transition. The smearing makes it very difficult to see small first-order discontinuities and the rounded jump in the order parameter will be mimicked by a power law with a low $\beta_{\rm eff}$ value [30]. In the case of the ammonium chlorides NH_4Cl and ND_4Cl, the first-order character is greater for NH_4Cl. The quantity $\Delta L/(\Delta L + \delta L) \simeq 0.27$ and the hysteresis was ~ 0.3 K for NH_4Cl, whereas $\Delta L/(\Delta L + \delta L) \simeq 0.15$ and the hysteresis was ~ 0.03 K for ND_4Cl, where ΔL is the first-order discontinuity in crystal length and $\Delta L + \delta L$ is the total change in length on ordering including pretransitional contributions above and below T_c [33]. The effective critical exponents were $\beta_{\rm eff} = 0.13 \pm 0.006$ [33] for both chlorides, $\alpha_{\rm eff} = 0.57 \pm 0.07$ for NH_4Cl, and $\alpha_{\rm eff} = 0.52$

± 0.07 for ND_4Cl [30,34]. In Ref. [30] it is shown that these effective experimental values are compatible with the tricritical values $\alpha = 0.5$ and $\beta = 0.25$ when inhomogeneous strains are present.

Our ''best'' values for 65OBC, $\alpha_{\text{eff}} = 0.65 \pm 0.05$ and $2\beta_{\text{eff}} = 0.35 \pm 0.05$ [3], are not very different from the NH_4Cl and ND_4Cl values cited above and seem marginally consistent with quasitricriticality in the Bergman-Halperin sense. Another possibility that should be mentioned is that the underlying critical point might be a Gaussian tetracritical point for which $\gamma = 1$, $\alpha = \frac{2}{3}$, and $\beta = \frac{1}{6}$. In this scenario, the Sm*A*-Hex*B* transition would be a quasitetracritical point, but there is no clear theoretical reason for such a point to describe the Sm*A*-Hex*B* strain-coupled transition.

Models that generate an isolated Sm*A*-Hex*B* tricritical point have already been proposed by Aharony *et al.* [19], who considered $\Psi\rho^2$ coupling between the phase of Ψ and positional density, and Selinger [35], who coupled the phase of Ψ to the smectic layer fluctuations u. However, it appears that a compressible XY model, i.e., an improved version of the Aeppli-Bruinsma model coupling Ψ to in-plane positional order [21] with fluctuations in the *amplitude* of Ψ taken into account and fluctuations allowed in the lateral strain in the spirit of the compressible n-vector model [27,31], is the most attractive direction for new theory. The deconvolved C_p data in Figs. 6 and 7 suggest that smearing due to strain inhomogeneties is limited to $T < T_c$, which seems natural since $\xi_\parallel$ is quite small (20–44 Å) in the Sm*A* phase and becomes large (55–$\sim$160 Å) in the Hex*B* phase [2,22]. It should be noted in passing that $\Delta C_p(\text{Sm}A\text{-Hex}B) \sim |t|^{-0.3}$ for two-layer films [6,24] and this ΔC_p behavior is in agreement with the behavior of the two-layer in-plane thermal expansion [36], both of which are completely incompatible with the theoretical expectations for a 2D XY system. However, taking in-plane strain coupling into account might be of significant importance.

The small C_p shoulder at about $T_c - 0.02$ K visible in Fig. 7 may well be related to a depressed transition occurring in disordered regions that are under an effective negative in-plane ''pressure'' due to the contraction associated with the increase in the in-plane q_0 and $\xi_\parallel$ as T is lowered below T_c. The slow annealing of this strain feature with time and with cycling through the transition, described in Sec. III, seems very reasonable for the picture of in-plane short-range but well-correlated regions ($\xi_\parallel \simeq 150-200$ Å) combined with regions that are more disordered. Comparable annealing of surface-induced strains with cycling has been observed for 65OBC [2(b)]. Note that the narrow and almost symmetrical peak in $C_{\text{app}}\sin\phi - (1/\omega R)$ achieved in late runs 11c and 12h has been interpreted as a region of two-phase coexistence due to the very weak first-order character to the 65OBC Sm*A*-Hex*B* transition.

In view of the absence of low-frequency dynamics for the Sm*A*-Hex*B* transition in 65OBC, the issue of the reported dynamics at the Sm*C*-Sm*I* critical point in a 8SI+8OSI mixture (methylbutyl phenyl octylbiphenyl-carboxylate and its octyloxybiphenyl analog) [8] should be reevaluated. Initial 65OBC experiments using a cell design like that employed in Ref. [8] yielded apparent dynamics for 65OBC that arose from thermal gradient effects at the standard operating frequency $\omega_0 = 0.196\ \text{s}^{-1}$ and above. A reanalysis [37] of the static limiting value $C_p(\omega = 0)$ for the critical 8SI+8OSI mixture indicates crossover behavior with data for $|t| > 7 \times 10^{-4}$ reasonably well described by Eq. (8) with $D_1^{\pm} \equiv 0$, $\alpha_{\text{eff}} \simeq 0.68$, $\Delta B_c \simeq 0.175$, and $A^-/A^+ \simeq 1.5$. The fitting parameters α_{eff} and ΔB_c are quite similar to those given for 65OBC in Table I, although the amplitude ratio differs. For 8SI+8OSI data in the range $\sim 7\times10^{-5} < |t| < 5\times10^{-4}$, the empirical critical exponent is about 0.93, the A^-/A^+ ratio is about 2.5, and ΔB_c is very close to zero.

It seems that the thermal conductivity K_s of hexatic liquid crystals must be quite low compared to typical thermotropic materials. Recent studies of two other systems, a blue phase III–isotropic critical point [12] and a second-order nematic (N)-Sm*A* transition [38], were carried out on the same calorimeter in cells like those used in Ref. [8] and in the initial 65OBC runs (1-mm-thick cell with gold wire). In both cases, $C_p(\omega)$ values agreed very well for all frequencies $\omega \leqslant \omega_0$. Many other smectic liquid crystals have shown no high-frequency rolloff effects at ω_0 in similar cells [9,39].

The singular behavior of K_s reported for 65OBC [4(c),6] is surprisingly different from the behavior observed at N-Sm*A* transitions, which are also in the 3D XY universality class [40]. Studies by Marinelli *et al.* [41] of 8CB and 8S5 have shown that K_s is nonsingular and essentially independent of T near $T_c(N\text{-Sm}A)$, i.e., the observed dip in the thermal diffusivity $D_T = K_s/\rho C_p$ is completely due to the peak in C_p for N-Sm*A* transitions.

V. SUMMARY

A high-resolution calorimetric study of the Sm*A*-Hex*B* transition in bulk 65OBC has revealed a very weak first-order character with a latent heat too small to measure with our techniques. The excess heat capacity $\Delta C_p(\text{Sm}A\text{-Hex}B)$ can be well described by $A^{\pm}|t|^{-\alpha_{\text{eff}}} + B_c$ with the critical exponent $\alpha_{\text{eff}} = 0.65 \pm 0.05$ and amplitude ratio $A^-/A^+ = 1.09 \pm 0.09$, but there are small systematic deviations unless $B_c^+ \neq B_c^-$ is allowed. This is just one of several indications of weak first-order behavior. Such a heat capacity exponent is dramatically different from the predicted 3D XY value $\alpha_{XY} = -0.007$, and the effective order-parameter exponent $\beta_{\text{eff}} = 0.17-0.19$ obtained from birefringence studies [3] also disagrees with $\beta_{XY} = 0.345$.

The limited available data suggest that the underlying critical behavior could be Gaussian, and it is proposed that this transition can be understood as *quasitricritical* or *quasitetracritical* where quasicritical is used in the same sense as Bergman and Halperin's result for a compressible Ising model [27]. Thus an appropriate theory would involve a compressible XY model [31] like the Aeppli-Bruinsma model [21] coupling Ψ to the in-plane positional short-range order but with fluctuations in the amplitude $|\Psi|$ and the strains explicitly taken into account in the spirit of Bergman and Halperin. Such a theoretical model would allow quasitricriticality (or perhaps quasitetracriticality) over a range of composition or a range of pressure for pure materials rather than an isolated tricritical point between first- and second-order regimes. This possibility of a range of quasicritical

behavior would conform to extensive experimental data on many hexatic materials [6].

ACKNOWLEDGMENTS

The authors wish to thank V. Surendranath of Kent State University, who synthesized and purified the 65OBC sample. We also thank C. C. Huang for helpful experimental discussions as well as G. Aeppli, A. Aharony, T. C. Lubensky, and D. Nelson for stimulating theoretical discussions. This work was supported in part by the National Science Foundation under Grant No. DMR 93-11853, MRSEC Grant No. DMR 94-00334, and STC-ALCOM Grant No. DMR 89-20147. Z.K. wishes to acknowledge support from the Fulbright program and the Ministry of Science of Slovenia.

[1] R. J. Birgeneau and J. D. Litster, J. Phys. (France) Lett. **39**, L399 (1978).

[2] (a) R. Pindak, D. E. Moncton, S. C. Davey, and J. W. Goodby, Phys. Rev. Lett. **46**, 1135 (1981); (b) J. W. Goodby and R. Pindak, Mol. Cryst. Liq. Cryst. **75**, 233 (1981).

[3] C. Rosenblatt and J. T. Ho, Phys. Rev. A **26**, 2293 (1982). Reference [14] of this paper states that the cited values $1-\alpha_{\rm eff}=0.40\pm0.05$ and $2\beta_{\rm eff}=0.38\pm0.05$ are maximum values and changes in the noncritical background would yield smaller values that lie within the error bounds. Thus $0.60<\alpha_{\rm eff}<0.65$ and $0.33<2\beta_{\rm eff}<0.38$ seem most likely.

[4] (a) C. C. Huang, J. M. Viner, R. Pindak, and J. W. Goodby, Phys. Rev. Lett. **46**, 1289 (1981); (b) J. M. Viner, D. Lamey, C. C. Huang, R. Pindak, and J. W. Goodby, Phys. Rev. A **28**, 2433 (1983); (c) G. Nounesis, C. C. Huang, and J. W. Goodby, Phys. Rev. Lett. **56**, 1712 (1986).

[5] J. C. LeGuillon and J. Zinn-Justin, J. Phys. (France) Lett. **46**, L137 (1985); C. Bagnuls and C. Bervillier, Phys. Rev. B **32**, 7209 (1985).

[6] C. C. Huang and T. Stoebe, Adv. Phys. **42**, 343 (1993), and references cited therein.

[7] R. Mahmood, M. Lewis, R. Biggers, V. Surendranath, D. Johnson, and M. E. Neubert, Phys. Rev. A **33**, 519 (1986); see also the discussion in R. Mahmood, M. Lewis, D. Johnson, and V. Surendranath, *ibid.* **38**, 4299 (1988).

[8] H. Yao, T. Chan, and C. W. Garland, Phys. Rev. E **51**, 4585 (1995).

[9] C. W. Garland, Thermochim. Acta **88**, 127 (1985).

[10] C. W. Garland, in *Liquid Crystals: Physical Properties and Phase Transitions*, edited by S. Kumar (Cambridge University Press, Cambridge, in press), Chap. 6.

[11] D. Finotello and G. S. Iannacchione, Int. J. Mod. Phys. B **9**, 2247 (1995).

[12] P. F. Sullivan and G. Seidel, Phys. Rev. **173**, 679 (1968). Internal thermal relaxation effects arising from finite sample thermal conductivity can be corrected for with Eqs. (1) and (2) for frequencies up to ~400 and ~62.5 mHz for the Kent State and MIT calorimeters, respectively. As the frequency is decreased from these values, the dominant thermal relaxation is that for heat flow from the sample plus cell to the bath, here the sample plus cell system acts like a single ''lump.'' The breakdown of the one-lump thermal model arises from the onset of thermal gradients at high enough frequencies where either the cell or sample or both can no longer follow the thermal oscillations. For the MIT cell design, two distinct thermal paths exist linking the thermometer and heater, one through the LC sample and another along the silver skin of the cell. The behavior of $T_{\rm ac}$ and ϕ can be modeled *qualitatively* by a parallel-path thermal model where heat flow through both paths are described separately by a one-lump model then combined as two parallel resistors. This approach can in principle justify the empirical use of a negative F value for correcting data at 31.75 and 62.5 mHz.

[13] A first-order transition with a tiny step in C_p and a qualitatively small latent heat was observed on cooling at ~329.1 K at MIT and at ~327 K at Kent State. This is presumably a transition between CrE and CrK, which is the stable form at room temperature. Note that CrK melts at ~338 K, so this transition is monotropic.

[14] Z. Kutnjak, C. W. Garland, C. G. Schatz, P. J. Collings, C. J. Booth, and J. W. Goodby, Phys. Rev. E **53**, 4955 (1996).

[15] C. W. Garland, G. Nounesis, M. J. Young, and R. J. Birgeneau, Phys. Rev. E **47**, 1918 (1993).

[16] R. Bruinsma and G. Aeppli, Phys. Rev. Lett. **48**, 1625 (1982).

[17] G. Nounesis, R. Geer, H. Y. Lui, C. C. Huang, and J. W. Goodby, Phys. Rev. A **40**, 5468 (1989).

[18] (a) E. Gorecka, L. Chen, O. Lavrentovich, and W. Pyzuk, Europhys. Lett. **27**, 507 (1994); (b) E. Gorecka, L. Chen, S. Kumar, A. Krowczynski, and W. Pyzuk, Phys. Rev. E **50**, 2863 (1994).

[19] A. Aharony, R. J. Birgeneau, J. D. Brock, and J. D. Litster, Phys. Rev. Lett. **57**, 1012 (1986).

[20] J. D. Brock, A. Aharony, R. J. Birgeneau, K. W. Evans-Lutterodt, J. D. Litster, P. M. Horn, G. B. Stephenson, and A. R. Tajbakhsh, Phys. Rev. Lett. **57**, 98 (1986); J. D. Brock, D. Y. Noh, B. R. McClain, J. D. Litster, R. J. Birgeneau, A. Aharony, P. M. Horn, and J. C. Liang, Z. Phys. B **74**, 197 (1989); these results pertain to the *tilted* SmC-SmI supercritical evolution in 8OSI (see Ref. [8]).

[21] G. Aeppli and R. Bruinsma, Phys. Rev. Lett. **53**, 2133 (1984).

[22] S. C. Davey, J. Budai, R. Pindak, J. W. Goodby, and D. E. Moncton, Phys. Rev. Lett. **53**, 2129 (1984). There is some uncertainty whether the Δq_0 amplitude ratio obtained here corresponds to the C_p amplitude ratio as claimed.

[23] T. Pitchford, C. C. Huang, R. Pindak, and J. W. Goodby, Phys. Rev. Lett. **57**, 1239 (1986).

[24] C. W. Garland and R. Renard, J. Chem. Phys. **44**, 1120 (1966); **44**, 1125 (1966); C. W. Garland and R. A. Young, *ibid.* **48**, 146 (1968).

[25] (a) A. J. Jin *et al.*, Phys. Rev. Lett. **74**, 4863 (1995); Phys. Rev. E **53**, 3639 (1996); (b) C.-F. Chou, J. T. Ho, S. W. Hui, and V. Surendranath, Phys. Rev. Lett. **76**, 4556 (1996); (c) J. T. Ho (private communication).

[26] J. L. Gallani, P. Martinoty, D. Guillon, and G. Poeti, Phys. Rev. A **37**, 3638 (1988).

[27] D. J. Bergman and B. I. Halperin, Phys. Rev. B **13**, 2145 (1976).

[28] P. E. Cladis and J. W. Goodby, Mol. Cryst. Liq. Cryst. **72**, 307 (1982).
[29] R. Pindak, W. O. Sprenger, D. J. Bishop, D. D. Osheroff, and J. W. Goodby, Phys. Rev. Lett. **48**, 173 (1982).
[30] K. J. Lushington and C. W. Garland, J. Chem. Phys. **72**, 5752 (1980), and references cited therein.
[31] M. A. deMoura, T. C. Lubensky, Y. Imry, and A. Aharony, Phys. Rev. B **13**, 2176 (1976).
[32] H. Haga and C. W. Garland (unpublished).
[33] B. B. Weiner and C. W. Garland, J. Chem. Phys. **56**, 155 (1972); C. W. Garland, D. E. Bruins, and T. J. Greytak, Phys. Rev. B **12**, 2759 (1975); D. E. Bruins and C. W. Garland, J. Chem. Phys. **63**, 4139 (1975).
[34] C. W. Garland and J. D. Baloga, Phys. Rev. B **16**, 331 (1977).
[35] J. V. Selinger, J. Phys. (France) **49**, 1387 (1988).
[36] T. Stoebe, C. C. Huang, and J. W. Goodby, Phys. Rev. Lett. **68**, 2944 (1992).
[37] H. Yao and C. W. Garland (unpublished).
[38] Z. Kutnjak and C. W. Garland, Phys. Rev. E **55**, 488 (1997).
[39] C. W. Garland, in *Phase Transitions in Liquid Crystals*, edited by S. Martellucci (Plenum, New York, 1992), Chap. 11, and references cited therein.
[40] C. W. Garland and G. Nounesis, Phys. Rev. E **49**, 2964 (1994).
[41] M. Marinelli, F. Mercuri, U. Zammit, and F. Scudiere, Phys. Rev. A **53**, 701 (1996); M. Marinelli, F. Mercuri, S. Foglietta, U. Zammit, and F. Scudieri, Phys. Rev. E **53**, 1604 (1996).